AIP | Physics of Plasmas
#1 JOURNAL IN 2014 GOOGLE SCHOLAR METRICS FOR THE PLASMA & FUSION CATEGORY

Influence of plasma density on the chemical composition and structural properties of pulsed laser deposited TiAlN thin films

J. G. Quiñones-Galván, Enrique Camps, S. Muhl, M. Flores, and E. Campos-González

Citation: Physics of Plasmas (1994-present) **21**, 053509 (2014); doi: 10.1063/1.4879025
View online: http://dx.doi.org/10.1063/1.4879025
View Table of Contents: http://scitation.aip.org/content/aip/journal/pop/21/5?ver=pdfcov
Published by the AIP Publishing

Articles you may be interested in

Effect of process parameters on properties of argon–nitrogen plasma for titanium nitride film deposition
J. Vac. Sci. Technol. A **31**, 061307 (2013); 10.1116/1.4821540

Deposition and composition-control of Mn-doped ZnO thin films by combinatorial pulsed laser deposition using two delayed plasma plumes
J. Appl. Phys. **112**, 044904 (2012); 10.1063/1.4747935

Preparation of α - Al 2 O 3 thin films by electron cyclotron resonance plasma-assisted pulsed laser deposition and heat annealing
J. Vac. Sci. Technol. A **26**, 380 (2008); 10.1116/1.2899569

The influence of the growth rate on the preferred orientation of magnetron-sputtered Ti–Al–N thin films studied by in situ x-ray diffraction
J. Appl. Phys. **98**, 044901 (2005); 10.1063/1.1999829

Raman spectroscopy and x-ray diffraction studies of (Ti,Al)N films deposited by filtered cathodic vacuum arc at room temperature
J. Appl. Phys. **89**, 6192 (2001); 10.1063/1.1352564

This article is copyrighted as indicated in the article. Reuse of AIP content is subject to the terms at: http://scitation.aip.org/termsconditions. Downloaded to IP: 132.248.12.211 On: Wed, 08 Apr 2015 18:13:08

PHYSICS OF PLASMAS 21, 053509 (2014)

Influence of plasma density on the chemical composition and structural properties of pulsed laser deposited TiAlN thin films

J. G. Quiñones-Galván,[1] Enrique Camps,[1] S. Muhl,[2] M. Flores,[3] and E. Campos-González[4]
[1]*Departamento de Física, Instituto Nacional de Investigaciones Nucleares, Apartado Postal 18-1027, México D.F. C.P. 11801, Mexico*
[2]*Instituto de Investigaciones en Materiales, UNAM, México D.F. C.P. 04510, Mexico*
[3]*Departamento de Ingeniería de Proyectos, CUCEI, Universidad de Guadalajara, Apdo. Postal 307, C.P. 45101 Zapopan, Jalisco, Mexico*
[4]*Departamento de Física, CINVESTAV-IPN, Apdo. Postal 14-740, México D.F. 07360, Mexico*

(Received 4 March 2014; accepted 7 May 2014; published online 22 May 2014)

Incorporation of substitutional Al into the TiN lattice of the ternary alloy TiAlN results in a material with improved properties compared to TiN. In this work, TiAlN thin films were grown by the simultaneous ablation of Ti and Al targets in a nitrogen containing reactive atmosphere. The deposit was formed on silicon substrates at low deposition temperature (200 °C). The dependence of the Al content of the films was studied as a function of the ion density of the plasma produced by the laser ablation of the Al target. The plasma parameters were measured by means of a planar Langmuir probe and optical emission spectroscopy. The chemical composition of the films was measured by energy dispersive X-ray spectroscopy. The results showed a strong dependence of the amount of aluminum incorporated in the films with the plasma density. The structural characterization of the deposits was carried out by Raman spectroscopy, X-ray diffraction, and transmission electron microscopy, where the substitutional incorporation of the Al into the TiN was demonstrated. © *2014 AIP Publishing LLC*. [http://dx.doi.org/10.1063/1.4879025]

I. INTRODUCTION

TiN thin films exhibit very interesting physical and chemical properties such as high hardness, good wear resistance, low friction coefficient, and elevated chemical inertness.[1] Additionally, the thermal stability, electric conductivity, and other characteristics, such as for diffusion barriers, make TiN an interesting material for many mechanical, decorative, thermal, and microelectronics applications, among others.[2] However, TiN has the disadvantage of forming the rutile phase TiO_2 at temperatures above 500 °C, and this causes significant degradation of the properties. The incorporation of different elements such as Si or Al into the TiN lattice has been demonstrated to be beneficial for the mechanical and tribological properties.[3–5] In particular, Al atoms can substitute Ti in the TiN lattice to form the ternary alloy TiAlN and this is of great interest because, as well as improving the mechanical and tribological properties; it also enhances the oxidation resistance of the material. Additionally, the thermal conductivity of TiAlN is lower than that of TiN, making the system TiAlN interesting for many applications such as coatings for high speed cutting tools. TiAlN thin films have been grown using a variety of physical vapor deposition (PVD) techniques: cathodic arc evaporation,[6,7] sputtering,[8–10] and laser ablation or pulsed laser deposition (PLD).[1] Growth of TiAlN has also been reported by chemical vapor deposition (CVD), where toxic gases are needed for the process.[11,12] The properties of TiAlN are strongly dependent on the Al amount, thus a precise control of the Al incorporation is required. For PVD processes, it is necessary to use multiple Ti-Al targets of different composition and this can be expensive. For the CVD processes, a precise control of the gas flow ratios, pressure, etc., is needed and this complicates the control of the Al content. Acquaviva *et al*. reported the growth of TiAlN thin films by means of laser ablation,[1] where they obtained polycrystalline films with a mixture of TiN and TiAlN phases.

Previously, the deposition of good quality TiN films oriented in the (111) or (200) by laser ablation has been reported by the present authors;[13] the preferential orientation was shown to depend on the plasma parameters used. In the present work, it was studied the combination of two plasmas produced by the simultaneous laser ablation of a Ti and an Al target in a reactive atmosphere containing nitrogen, and the influence of the plasma density on the chemical composition and structural properties of TiAlN thin films. Moreover, with this arrangement, there is no need for the fabrication of a set of targets with different compositions, in order to change the composition of deposited films. As will be shown, the variation of the density of the plasma of one of the targets (Al in this case) allows varying the composition of the deposited films.

II. EXPERIMENTAL

The experiments were carried out in a vacuum chamber evacuated to a base pressure of 2.6×10^{-4} Pa with a turbomolecular pump. During the deposition, the chamber was backfilled with a gas mixture of 60/40 Ar/N_2 to a working pressure of 1.06 Pa. For the ablation process, a Nd:YAG laser with 500 mJ of maximum output energy, a wavelength of 1064 nm, 5 ns pulse width, and frequency of 10 Hz was used. The TiAlN thin film depositions were carried out by simultaneous ablation of high purity Ti and Al targets (2.54 cm in diameter), which were rotated at 15 rpm during the ablation process in order to avoid drilling of the target. The Ti target was placed 6 cm in front of, and parallel to the

 © 2014 AIP Publishing LLC

This article is copyrighted as indicated in the article. Reuse of AIP content is subject to the terms at: http://scitation.aip.org/termsconditions. Downloaded to IP: 132.248.12.211 On: Wed, 08 Apr 2015 18:13:08

substrate, while the Al target was placed between, and below, the Ti target and the substrate. The distance from the ablation point on the aluminum target and the central part of the substrate was varied between 2.5 and 5 cm, see Figure 1. The laser beam was divided into two equal beams, one directed towards the Ti target and the other to the Al target. The films were deposited on silicon substrates at a temperature of 200 °C.

The incident energy density on the Ti target was kept constant at 7 J/cm^2 in order to have a constant mean kinetic energy of the ions and plasma density from the Ti target. These conditions were chosen for the Ti ablation since they had been shown to produce good quality TiN films oriented in the (111) direction.[13] For the case of the Al target, the incident energy density and the distance to the substrate were varied (2.5–5 cm) such that the plasma density was varied, whilst the energy of the ions was kept approximately constant at 100 eV. The deposition time was adjusted to give a sample thickness of approximately 700 nm for all the deposition conditions.

Optical emission spectroscopy (OES) of the discharges was performed using a 0.5 m spectrograph (Spectra Pro 500i) equipped with a fast intensified charge-coupled device (ICCD) for detection. The light emitted by the plasma was collected by a system of lenses and focused on a quartz optical fiber bundle, and transported to the spectrograph. The OES measurements were used in order to determine the type of excited species generated during the ablation of the targets; using standard references.[14,15]

The plasma parameters, mean kinetic ion energy and plasma density, were measured by the time of flight technique (TOF) using a 6 mm diameter planar Langmuir probe biased at −50 V; a value at which the ion current to the probe was saturated. For these measurements, the substrate was replaced by the planar probe in the exact position of the substrate. The probe current was obtained by measuring the voltage drop across a 15 Ω resistor; this voltage was measured using a Tektronix 500 MHz digital oscilloscope. The planar Langmuir probe was placed 6 cm in front of the Ti target (which also was the position of the substrate). The probe measurements gave TOF curves of the ions and from these using the procedure described by Bulgakova *et al.*, it was possible to calculate the average kinetic energy of the ions, E_k, present in the plasma.[16] The calculation uses the following relationship:

$$\langle E_k \rangle = \frac{mL^2}{2} \frac{\int_0^T t^{-2} I(t)dt}{\int_0^T I(t)dt},$$

where m is the mass of the ion, L is the target to probe distance, and I(t) is the probe current as a function of time. The plasma density was calculated from the maximum value of current of the TOF curves.[17] For the experiments reported in this work, the mean kinetic ion energy and plasma density, of the particles produced from the Ti target, were kept constant at values of 300 eV and 1.4×10^{17} m^{-3}, respectively. The mean kinetic energy of the particles produced from the Al target, was approximately 100 eV for all the experiments and the plasma density was varied from 9×10^{15} up to 43×10^{15} m^{-3}. The distance of the substrate from the aluminum target, D_{Al}, was varied from 2.5 up to 5 cm, and this was used to produce the changes in the plasma density. The laser fluence on the aluminum target was varied using attenuators in order to keep the ion energy constant. All the measurements of the aluminum target plasma characteristics were obtained without ablation of the titanium target and vice versa for the titanium target plasma.

The chemical composition of TiAlN thin films was measured using an Oxford 3608 Energy Dispersive Spectroscopy (EDS) equipment installed in a JEOL 5900LV scanning electron microscope (SEM). The structural properties were analyzed by X-ray diffraction (XRD), Raman spectroscopy, and transmission electron microscopy (TEM). For the XRD measurements, a Siemens D-5000 diffractometer was used. The Raman spectroscopy measurements were carried out on a Horiba Jobin Yvon HR 800 Raman spectrometer with the 532 nm excitation line, the beam was focused using a 50× objective lens. The TEM measurements of the samples were made using a Jeol JEM 2010 microscope with a lanthanum hexaboride filament at an acceleration voltage of 200 kV.

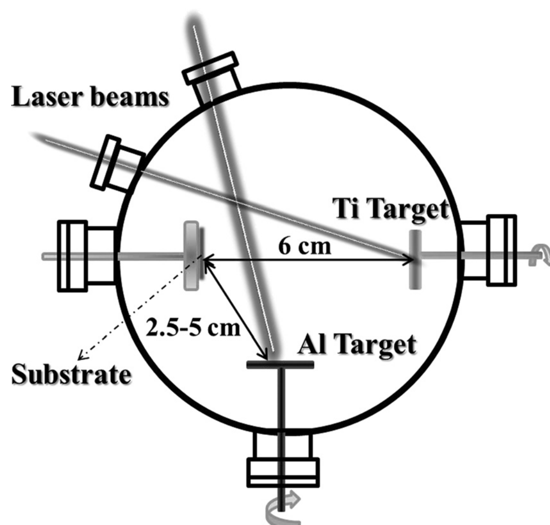

FIG. 1. A schematic diagram of the PLD system.

III. RESULTS AND DISCUSSION

Figure 2 shows the typical OES spectra of the plasma formed during the ablation of the titanium target (Fig. 2(a)) and the aluminum target (Fig. 2(b)). These spectra were obtained using the following experimental conditions: the distance between the titanium target and the position of the substrate was 6 cm, the aluminum target was located at 2.5 cm from the central part of the substrate and the gas pressure was 1.06 Pa (of the gas mixture 60/40 Ar/N_2). The laser fluence on the Ti and the Al targets were 7 and 6 J/cm^2, respectively. The observation point for the light emitted by the plasma was close to the substrate position.

In the spectrum of the plasma formed by the ablation of the Ti target, we observed the presence of neutral excited titanium (Ti) and singly ionized titanium (Ti^+). Figure 2(a) shows the spectral region, where the most intense emission

This article is copyrighted as indicated in the article. Reuse of AIP content is subject to the terms at: http://scitation.aip.org/termsconditions. Downloaded to IP: 132.248.12.211 On: Wed, 08 Apr 2015 18:13:08

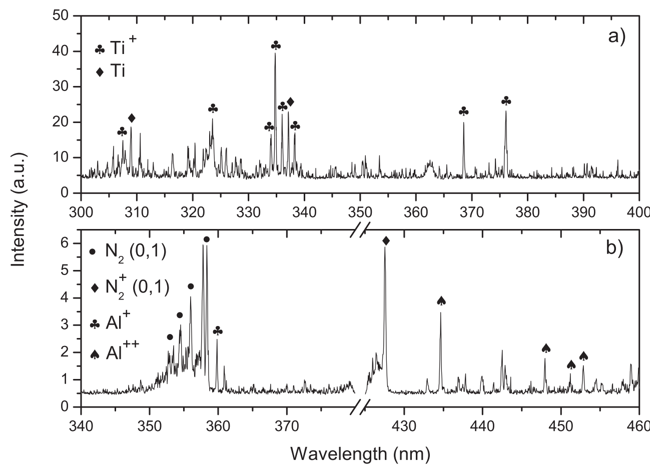

FIG. 2. Optical emission spectra of the plasma produced by laser ablation of the; (a) Ti target and (b) Al target, at the gas pressure used for all the experiments.

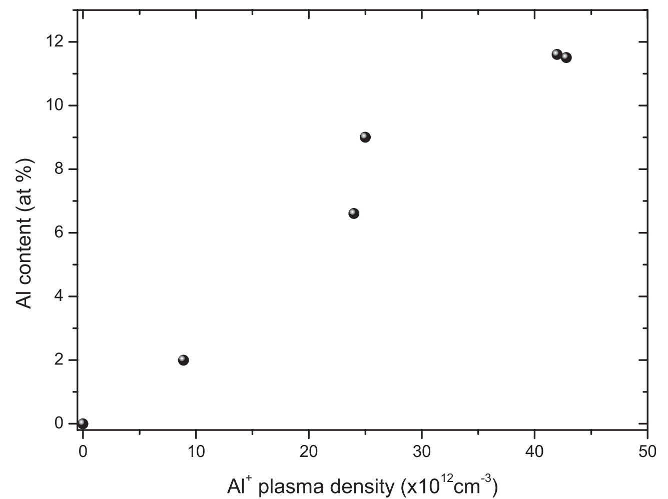

FIG. 4. The Al content as a function of aluminum plasma density.

peaks were detected; this spectrum was measured 2 μs after the interaction of the laser beam with the target (delay time), where the maximum of emission was observed. It is worth noting that no emission lines from the background gases were detected. Figure 2(b) shows the emission peaks of the plasma produced during the ablation of the aluminum target with 200 ns of delay time, again where the emission maximum occurred. We observed the presence of singly and doubly ionized excited aluminum (Al^{+}, Al^{++}), and neutral and singly ionized excited molecular nitrogen (N_2 and N_2^{+}). When both targets were simultaneously ablated the emission was a sum of the individual spectra; however, the titanium species were the most intense. There was no detected emission of molecules, such as AlN or TiN, even up to 5 μs of delay time when all emission stopped.

Figure 3 shows the data obtained from the TOF measurements of the plasma plume; Fig. 3(a) shows data for the ablation of the Ti target; and Fig. 3(b) shows data for the Al target for the different experimental conditions. The graphs also contain the values of the plasma density for each experiment. As mentioned earlier, the average ion energy and plasma density of the Ti plasma were kept constant at 300 eV and 1.14×10^{14} cm^{-3}, respectively, and for the ablation of the aluminum target the target-to-probe (target-to-substrate) distance was varied such that the average ion energy was close to 100 eV for all the experiments. However, in this case, the plasma density was varied from 9×10^{12} to 43×10^{12} cm^{-3}. The calculations of the plasma density used the maximum current of the TOF curves for each experiment and the average ion energy, $\langle E_k \rangle$, was obtained as described in Sec. II.

The change in plasma density during ablation of the aluminum target (for simplicity we called this the aluminum plasma) affects the Al content on the TiAlN thin films. Fig. 4 shows the Al concentration in the deposited thin films, as measured by EDS, as a function of Al plasma density. A linear dependence of Al content on plasma density can be observed as the amount of Al was increased from 2 up to ~12 at. %.

Raman spectroscopy was used to qualitatively observe the effects of the Al incorporation in the TiN lattice. Under lattice distortion, the Raman modes of TiN would be

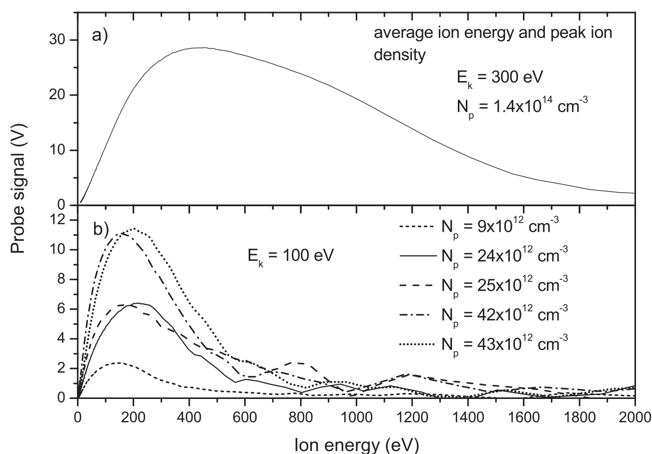

FIG. 3. The data from the TOF measurements obtained using the Langmuir probe is presented as the probe signal versus the energy of the corresponding ion; (a) the Ti plasma and (b) the Al plasma for different laser ablation conditions. The shown values of the mean kinetic energy of ions (E_k) and the plasma density (N_p) were calculated from the data.

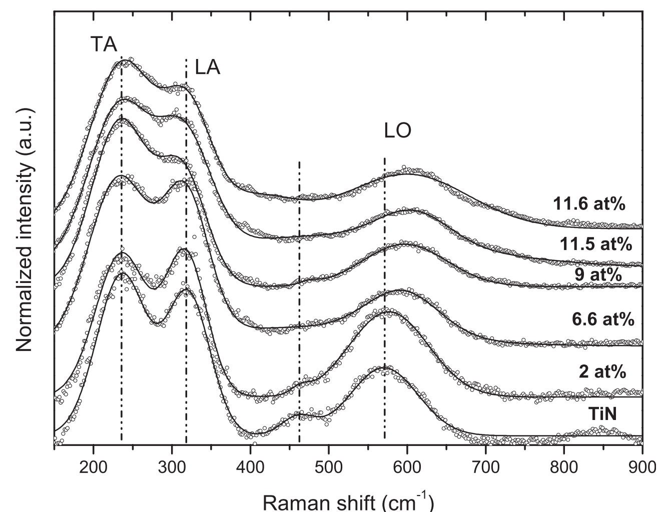

FIG. 5. Raman spectra of TiAlN thin films with different aluminum contents.

This article is copyrighted as indicated in the article. Reuse of AIP content is subject to the terms at: http://scitation.aip.org/termsconditions. Downloaded to IP: 132.248.12.211 On: Wed, 08 Apr 2015 18:13:08

expected to shift. Figure 5 presents the Raman spectra of a reference TiN sample and of the TiAlN thin films with different Al contents. Three of the characteristic features of TiN can be seen in all the spectra; the bands below 400 cm^{-1} are associated with the transverse (TA 236 cm^{-1}) and longitudinal acoustic (LA 320.6 cm^{-1}) phonons, while the band near 570 cm^{-1} is due to the optical phonons (LO 570.3 cm^{-1}). The TA band did not shift significantly as Al was incorporated in the films. However, the LA band was shifted to lower frequencies and the intensity of this band decreases with the addition of Al. When the Al content was increased the LO band shifted to higher frequencies and the intensity decreased. Table I shows the position of the LA and LO bands and their intensities for the different Al contents in the films. Similar Raman shifts to higher frequencies when Al is added to TiN have been previously reported.[18,19] The decrease in intensity of the LA and LO modes could be explained by a decrease in the number of Ti-N bonds when Al is incorporated, with this suggesting that Al atoms substitute Ti atoms in the TiN lattice.

On the other hand, the shift of the LO band towards higher values could be explained as the formation of a higher concentration of Al-N bonds as the Al content in the films increased. The vibrations of the Al-N bonds are located at 614, 660, and 673 cm^{-1}.[20] In the case of the deposited films in this work, the LO band can be fitted with two Gaussian curves, one of them centered at 570 cm^{-1}, and the other one at higher values of the Raman shift, in particular, for the case of the sample with an aluminum content of 11.6 at. %, this second curve is centered at 657 cm^{-1}, which strongly supports the idea of the formation of Al-N bonds.

In order to analyze the incorporation of Al into the TiN lattice, XRD measurements were performed. Figure 6 shows the XRD patterns of a TiN reference sample and those of the samples with 2 and 11.6 at. % of Al. The intensity of the peaks was adjusted so that the displacement of the peaks could be clearly observed. Only a single peak was present in all the diffraction patterns. The peak of the reference TiN was centered at $2\theta = 36.02°$ and corresponds to the (111) direction of TiN. As the Al content in the films increased, the diffraction peaks moved towards higher values of 2θ. For the case of 2 at. % and 11.6 at. % samples, the diffraction peak was centered at 36.34° and 36.73°, respectively. The diffraction data were used to calculate the lattice parameters of the different samples, and the results are plotted in Fig. 7.

TABLE I. Raman peak positions and intensities of the LA and LO modes for the samples with different aluminum concentrations.

	LA		LO	
Al content (at. %)	Raman shift (cm^{-1})	Intensity (a.u.)	Raman shift (cm^{-1})	Intensity (a.u.)
0	320.6	0.81	570.3	0.39
2.0	317.6	0.81	576.4	0.49
6.6	317.3	0.80	594.0	0.25
9.0	313.0	0.65	596.6	0.24
11.5	319.8	0.61	599.7	0.31
11.6	315.0	0.66	608.6	0.18

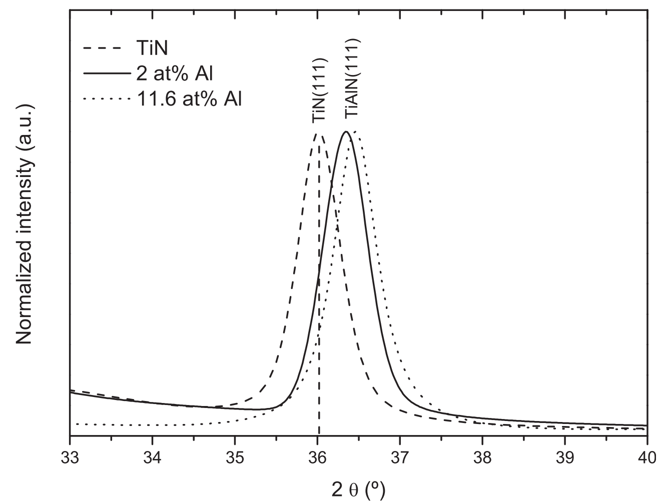

FIG. 6. XRD patterns of representative samples. The dashed line corresponds to the (111) plane of TiN.

As can be seen, the lattice parameter decreased as the Al content increased. The atomic radius of Al is less than that of Ti; therefore, the observed shrinkage of the lattice parameter agrees with the idea that Ti is substituted by Al as the Al concentration increased.

A very thin film was deposited on a NaCl substrate using a plasma density of 45×10^{12} cm^{-3} (according to the data shown in Fig. 4 this corresponded to the highest Al content, ~11.5 at. %, in the films). The film thickness was estimated to be approximately 55 nm according to the deposition rates for samples grown on similar conditions (5.5 nm/s). The substrate was then dissolved in water and the film was collected on a TEM grid, in order to obtain high resolution TEM images. Figure 8 shows a micrograph of the TiAlN thin film, the square box shows the planes corresponding to the (111) direction of TiN. The interplanar distance of these planes is $d = 2.444 \pm 0.007$ Å and this gives a lattice parameter value of $a = 4.232 \pm 0.012$ Å, which is smaller than the lattice parameter of TiN ($a = 4.315$ Å). The value of the lattice parameter is very close to that obtained from the X-ray diffraction measurements of the normal thickness samples prepared

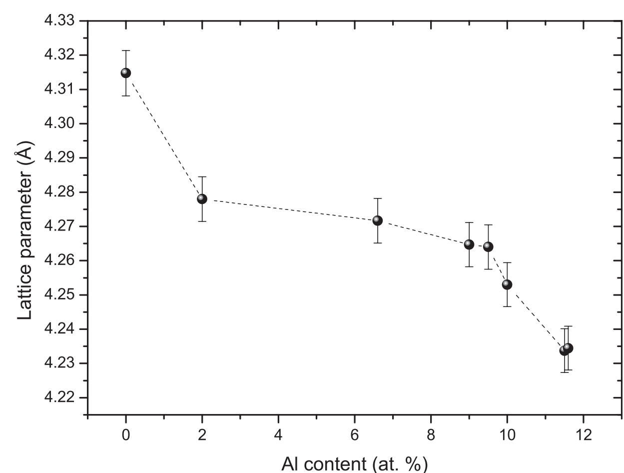

FIG. 7. The variation of the lattice parameter with the aluminum content. The dashed line is a guide for the eye.

This article is copyrighted as indicated in the article. Reuse of AIP content is subject to the terms at: http://scitation.aip.org/termsconditions. Downloaded to IP: 132.248.12.211 On: Wed, 08 Apr 2015 18:13:08

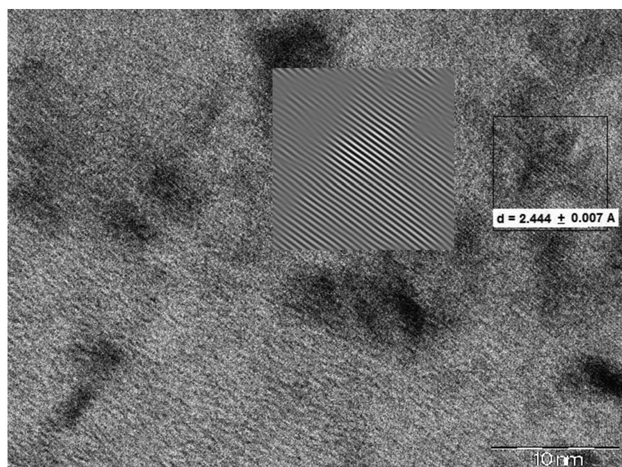

FIG. 8. A transmission electron micrograph of a TiAlN sample. The inset is a reconstruction of the planes observed in the area enclosed in the box.

using the same plasma density (see Fig. 7). Extensive examination of the TEM images showed no evidence of the existence of precipitation of aluminum, or crystals of aluminum, in the deposit and this again supports our hypothesis that the aluminum substitutes the titanium in the TiN crystal lattice.

IV. CONCLUSIONS

TiAlN thin films were prepared by means of the simultaneous ablation of Ti and Al targets in nitrogen containing reactive atmosphere. It was shown that the chemical composition of the films was strongly dependent on the ion plasma density. Additionally, from the results we believe that aluminum was incorporated into the TiN lattice by substitution of Ti by Al. Certainly for aluminum concentrations less than 12 at. %, there was no evidence of the existence of aluminum precipitation. From 0 to ~12 at. %, the amount of aluminum can be precisely controlled by controlling the plasma density. Even though OES showed the presence of nitrogen ions the results indicated that, under the experimental conditions studied, the concentration of aluminum ions in the Al plasma is directly proportional to the plasma density.

ACKNOWLEDGMENTS

This work was partially supported by CONACYT under Contract No. 128732.

[1]S. Acquaviva, E. D'Anna, L. Elia, M. Fernández, G. Leggieri, A. Luches, M. Martino, P. Mengucci, and A. Zocco, Thin Solid Films **379**, 45 (2000).
[2]L. García-González, M. G. Garnica-Romo, J. Hernández-Torres, and F. J. Espinoza-Beltrán, Braz. J. Chem. Eng. **24**(2), 249 (2007).
[3]L. Chen, Y. Du, S. Q. Wang, A. J. Wang, and H. H. Xua, Mater. Sci. Eng., A **502**, 139 (2009).
[4]C. L. Chang, W. C. Chen, P. C. Tsai, W. Y. Ho, and D. Y. Wang, Surf. Coat. Technol. **202**, 987 (2007).
[5]S. Veprek and M. J. G. Veprek-Heijman, Surf. Coat. Technol. **202**, 5063 (2008).
[6]Z. Hui, W. Xiao-hui, L. Qiu-lei, C. Li-jia, and L. Zheng, Trans. Nonferrous Met. Soc. China **20**, s679 (2010).
[7]Ch. Wüstefeld, D. Rafaja, M. Dopita, M. Motylenko, C. Baehtz, C. Michotte, and M. Kathrein, Surf. Coat. Technol. **206**, 1727 (2011).
[8]F. Jose, R. Ramaseshan, A. K. Balamurugan, S. Dash, A. K. Tyagi, and B. Raj, Mater. Sci. Eng., A **528**, 6438 (2011).
[9]M. Gîrleanu, M.-J. Pac, P. Louis, O. Ersen, J. Werckmann, C. Rousselot, and M.-H. Tuilier, Thin Solid Films **519**, 6190 (2011).
[10]F. Jose, R. Ramaseshan, S. Dash, S. T. Sundari, D. Jain, V. Ganesan, P. Chandramohan, M. P. Srinivasan, A. K. Tyagi, and B. Raj, Mater. Chem. Phys. **130**, 1033 (2011).
[11]S. Ikeda, S. Gilles, and B. Chenevier, Thin Solid Films **315**, 257 (1998).
[12]C. W. Kim and K. H. Kim, Thin Solid Films **307**, 113 (1997).
[13]L. Escobar-Alarcón, E. Camps, M. A. Castro, S. Muhl, and J. A. Mejia-Hernandez, Appl. Phys. A **81**, 1221 (2005).
[14]R. W. B. Pearse and A. G. Gaydon, *The Identification of Molecular Spectra* (John Wiley & Sons, 1976).
[15]A. Kramida, Yu. Ralchenko, J. Reader, and NIST ASD Team, *NIST Atomic Spectra Database*, National Institute of Standards and Technology, Gaithersburg, MD, USA. See http://physics.nist.gov/asd.
[16]N. M. Bulgakova, A. V. Bulgakov, and O. F. Bobrenok, Phys. Rev. E **62**, 5624 (2000).
[17]B. Doggett and J. G. Lunney, J. Appl. Phys. **105**, 033306 (2009).
[18]C. P. Constable, J. Yarwood, and W.-D. Münz, Surf. Coat. Technol. **116**, 155 (1999).
[19]H. C. Barshilia and K. S. Rajam, J. Mater. Res. **19**(11), 3196 (2004).
[20]L. E. McNeil, M. Grimsditch, and R. H. French, J. Am. Ceram. Soc. **76**, 1132 (1993).

This article is copyrighted as indicated in the article. Reuse of AIP content is subject to the terms at: http://scitation.aip.org/termsconditions. Downloaded to IP: 132.248.12.211 On: Wed, 08 Apr 2015 18:13:08